Electronic Supplementary Information for

Capture and characterization of elusive cyclo-di-BADGE

Fatemeh Salami,[a] Jian-bin Lin,[b] Bing Chen,[c] Baiyu H. Zhang[d] and Yuming Zhao[a*]

[a]Department of Chemistry, Memorial University, Core Science Facility, 45 Arctic Avenue, St. John's, NL, Canada A1C 5S7

[b]Centre for Chemical Analysis, Research and Training (C-CART), Core Science Facility, 45 Arctic Avenue, St. John's, NL, Canada A1C 5S7

[c]Northern Region Persistent Organic Pollutant Control (NRPOP) Laboratory, Faculty of Engineering and Applied Science, Memorial University, St. John's, NL Canada A1B 3X5

Table of Contents

1. Crystallization and Purification Procedures for Cyclo-di-BADGE

1.1 Crystallization of cyclo-di-BADGE

Single crystals of cyclo-di-BADGE were obtained during the purification step of the following synthetic reaction. First, a condensation reaction was performed as described in Scheme S-1. After 4 hours of reaction at 110 °C, the reaction mixture was cooled down to room temperature and then worked up through flash silica column chromatography using ethyl acetate and hexanes (9:1, v/v) as the eluent. It was at this stage where the cyclo-di-BADGE was introduced into the system.

The crude products were found to contain a variety of polar PHAs, mostly unreacted starting materials (**1**–**3**) and the condensation product (**4**) as outlined in Scheme S-1. In an attempt to crystallize the major product(s) from THF/methylene chloride (2:1, v/v), a few pieces of colorless single crystals were picked up, which was later proven to be cyclo-di-BADGE by X-ray analysis.

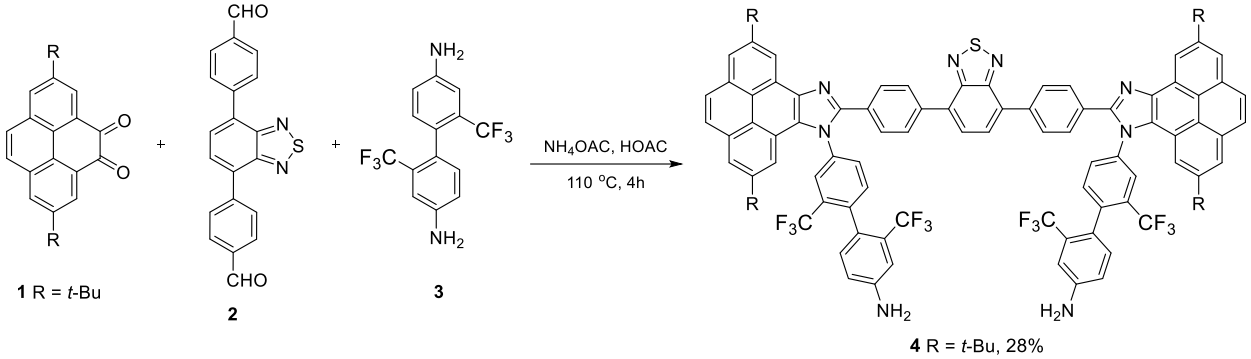

Scheme S-1 A condensation reaction to produce pyrenoimidazole derivative **4** using pyrenedione as one of the precursors.

1.2 Purification of cyclo-di-BADGE

Bulk ethyl acetate (1.5 L) that was contaminated with cyclo-di-BADGE was evaporated by distillation. The resulting crude cyclo-di-BADGE was an oily residue, which was dissolved in dichloromethane (10 mL). To this solution was added hexanes (100 mL) as an anti-solvent. Colorless precipitates were formed and collected through vacuum filtration. The obtained solid sample was further purified through rinsing with diethyl ether (15 mL × 3) at room temperature to remove aliphatic impurities. After this treatment, pure cyclo-di-BADGE (~100 mg) was obtained as colorless powder.

2. Characterizations of Cyclo-di-BADGE

2.1 FT-IR analysis of cyclo-di-BADGE

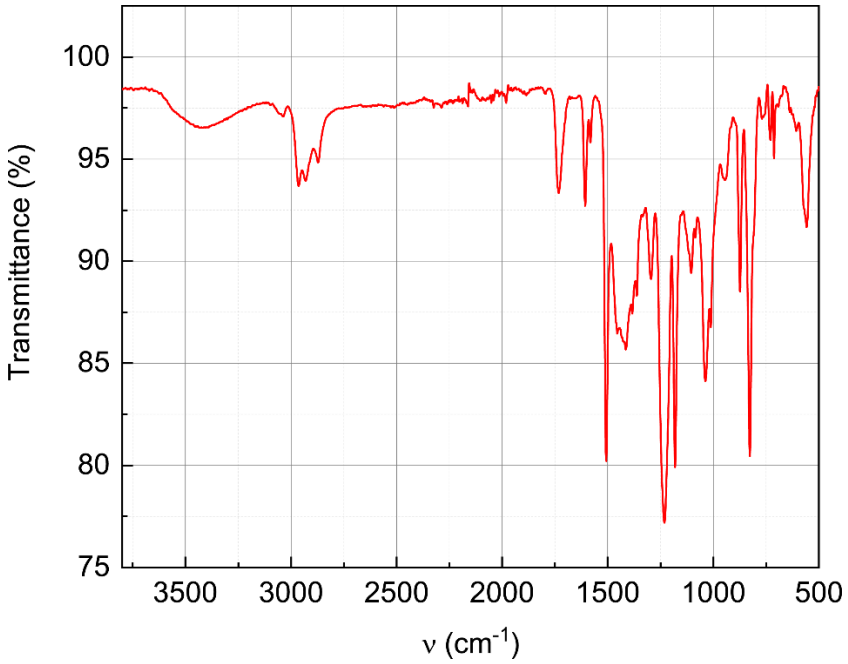

Fig. S-1 FT-IR spectrum of cyclo-di-BADGE.

2.2 NMR Spectroscopic analysis of cyclo-di-BADGE

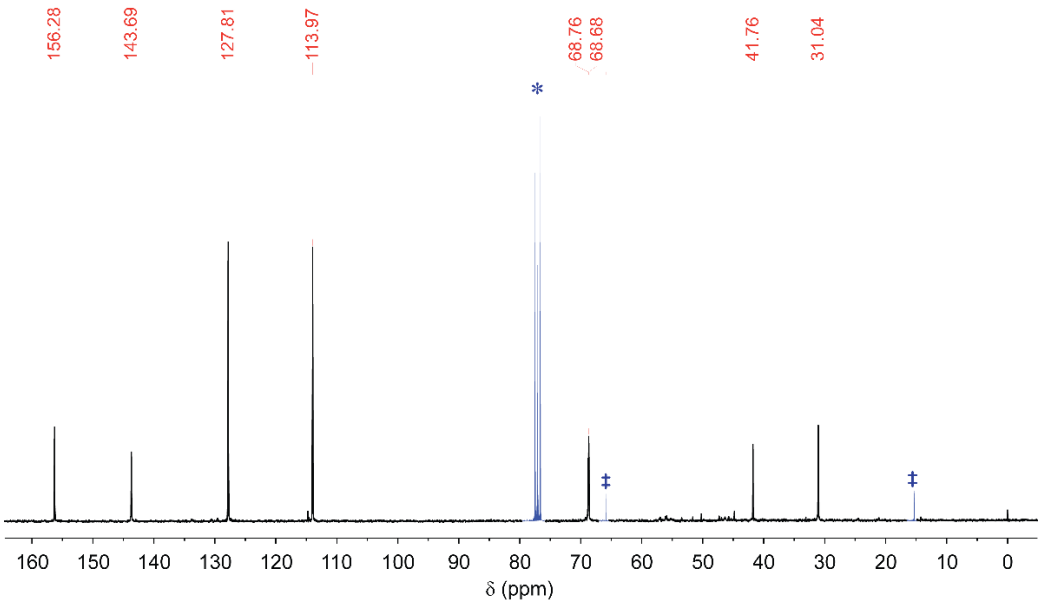

Fig. S-2 ^{13}C NMR (75 MHz, $CDCl_3$) of cyclod-di-BADGE. Solvent signals are indicated (*$CDCl_3$, and ‡diethyl ether).

2.3 UV-Vis analysis of cyclo-di-BADGE

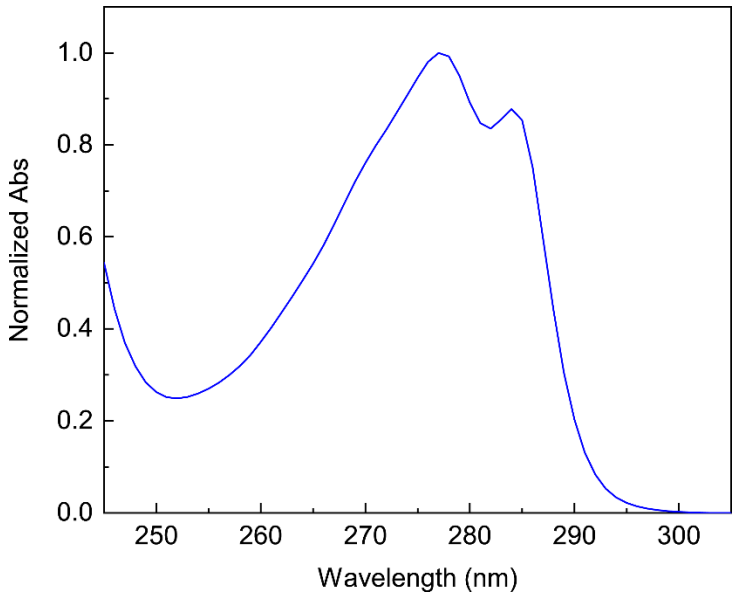

Fig. S-3 Normalized UV-Vis absorption spectrum of cyclo-di-BADGE measured in DMSO.

2.4 X-ray single crystallographic data for cyclo-di-BADGE

Table S-1. Crystal data and structure refinement

Identification code	cyclo-di-BADGE
Empirical formula	$C_{36}H_{40}O_6$
Formula weight	568.68
Temperature/K	100(2)
Crystal system	monoclinic
Space group	$P2_1/c$
a/Å	12.5112(2)
b/Å	24.0500(3)
c/Å	11.0199(2)
α/°	90
β/°	101.0650(10)
γ/°	90
Volume/Å^3	3254.18(9)
Z	4
ρ_{calc}g/cm^3	1.161
μ/mm^{-1}	0.625
F(000)	1216.0
Crystal size/mm^3	0.094 × 0.086 × 0.058
Radiation	Cu $K\alpha$ (λ = 1.54184)

2θ range for data collection/°	7.352 to 158.698
Index ranges	$-15 \leq h \leq 15$, $-24 \leq k \leq 30$, $-13 \leq l \leq 14$
Reflections collected	33581
Independent reflections	6895 [R_{int} = 0.0454, R_{sigma} = 0.0344]
Data/restraints/parameters	6895/0/452
Goodness-of-fit on F^2	1.091
Final R indexes [I>=2σ (I)]	R_1 = 0.0700, wR_2 = 0.1675
Final R indexes [all data]	R_1 = 0.0802, wR_2 = 0.1734
Largest diff. peak/hole / e Å^{-3}	0.34/-0.30

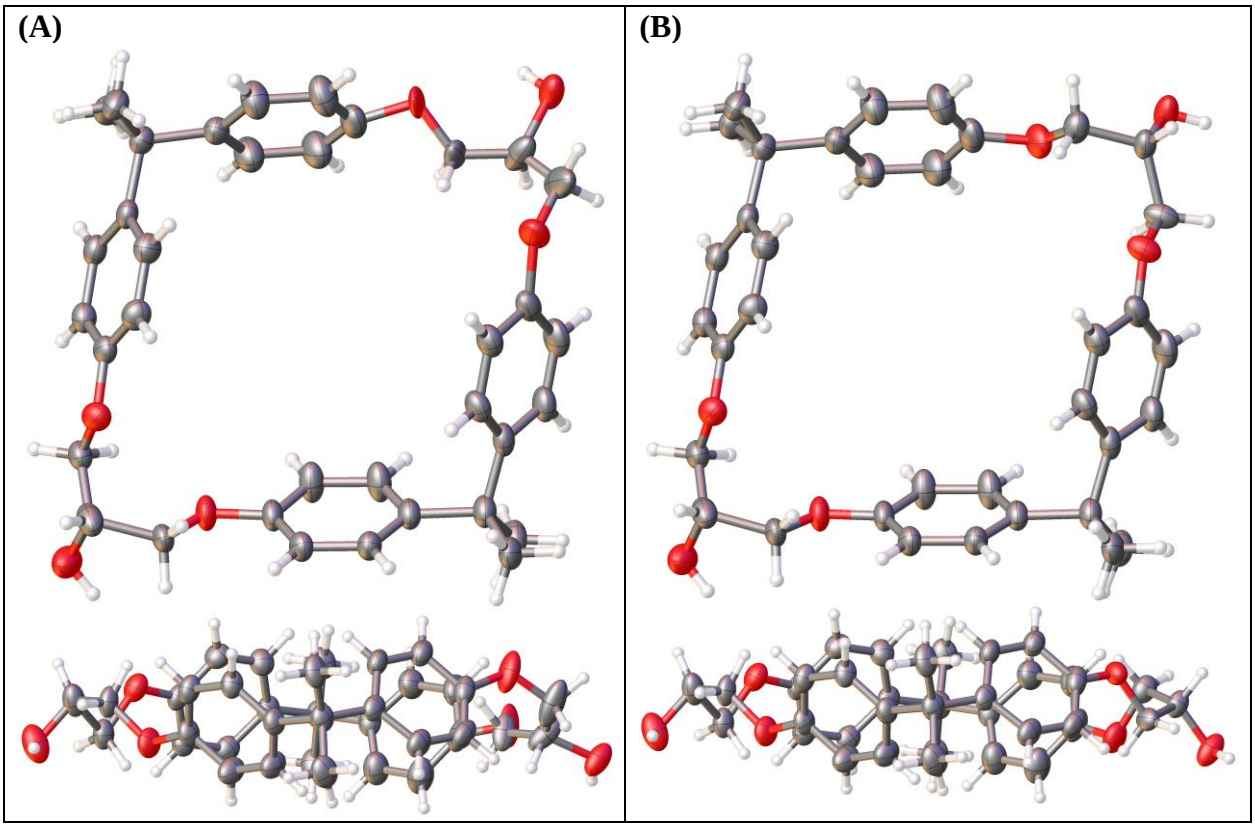

Fig. S-4 Front and side views of two molecular structures of cyclo-di-BADGE determined in the crystal structure. (A) a *trans* isomer accounting for 3.72% of population. (B) a *cis* isomer account for 11.0% of population.

3. Experimental Procedures for the Titration of BSA with Cyclo-di-BADGE

Bovine serum albumin (BSA, pH 7, > 98%) was acquired from Sigma Aldrich. A phosphate-buffered saline (PBS) solution (pH 7.4) was prepared by dissolving NaCl (0.137 M), Na_2HPO_4 (0.01 M), KCl (0.0027 M), and KH_2PO_4 (0.0018 M) in millipore purified water. To the PBS buffer solution was added with BSA (49.68 μM), and the resulting BSA solution was titrated with cyclo-di-BADGE. The steps of titration were monitored by UV-Vis (see Fig. S-4) and fluorescence spectral analyses (see Fig. 14 in the main context), respectively.

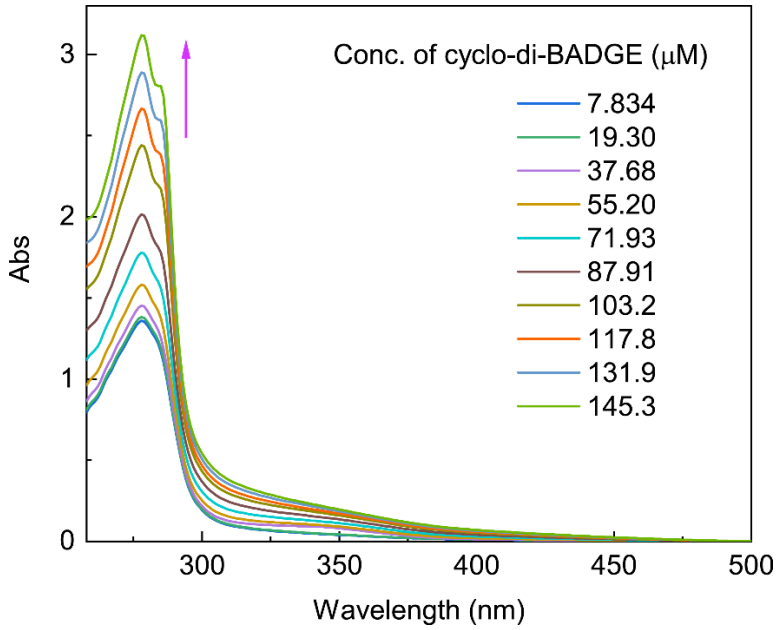

Fig. S-5 UV-Vis titration of BSA (49.68 mM) with cyclo-di-BADGE in a PBS solution at room temperature.

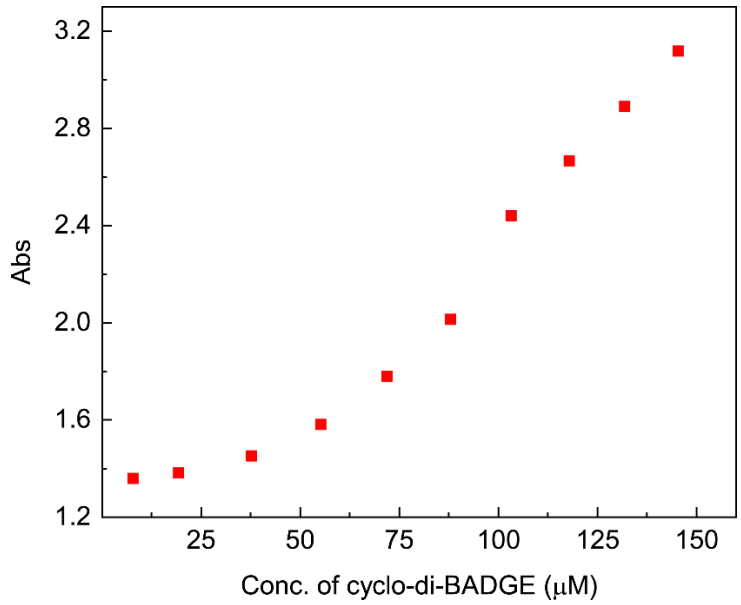

Fig. S-6 Plot of absorbance at 278 nm with the concentration of cyclo-di-BADGE from the titration of BSA (49.68 mM) with cyclo-di-BADGE in a PBS solution at room temperature. The correlation shows deviation from linearity, which is indicative of the binding of BSA with cyclo-di-BADGE.

4. Conformational Analysis of Cyclo-di-BADGE by CREST/DFT Modeling

The molecular structure of *cis* and *trans* cyclo-di-BADGE were first optimized using the GFN2-xTB program. The optimized structures were next subjected to CREST conformational analysis. A total of 973 conformers were obtained from the CREST calculations on *cis* cyclo-di-BADGE. The interatomic distance between the two dimethyl-substituted carbons in each of the structures is defined as the diagonal distance (*D*). The *D* values of all the conformers were extracted using a function integrated in the program, Multiwfn 3.7 (Lu, T.; Chen, F. *J. Comput. Chem*. **2012**, *33*, 580-592).

Fig. S-7 shows a statistical analysis of the *D* of these conformers in correlation with their relative energies (rel. *E*). In this plot, the open-shaped conformers with the *D* values greater than 10.1 Å are highlighted, which represent structures resembling those determined in the X-ray analysis. Similarly, the structural analysis of the *trans* cyclo-di-BADGE conformers calculated by CREST is summarized in Fig. S-8. Comparison of Fig. S-7 and Fig. S-8 indicates that *trans* cyclo-di-BADGE affords a larger number of open-shaped conformers than *cis* cyclo-di-BADGE.

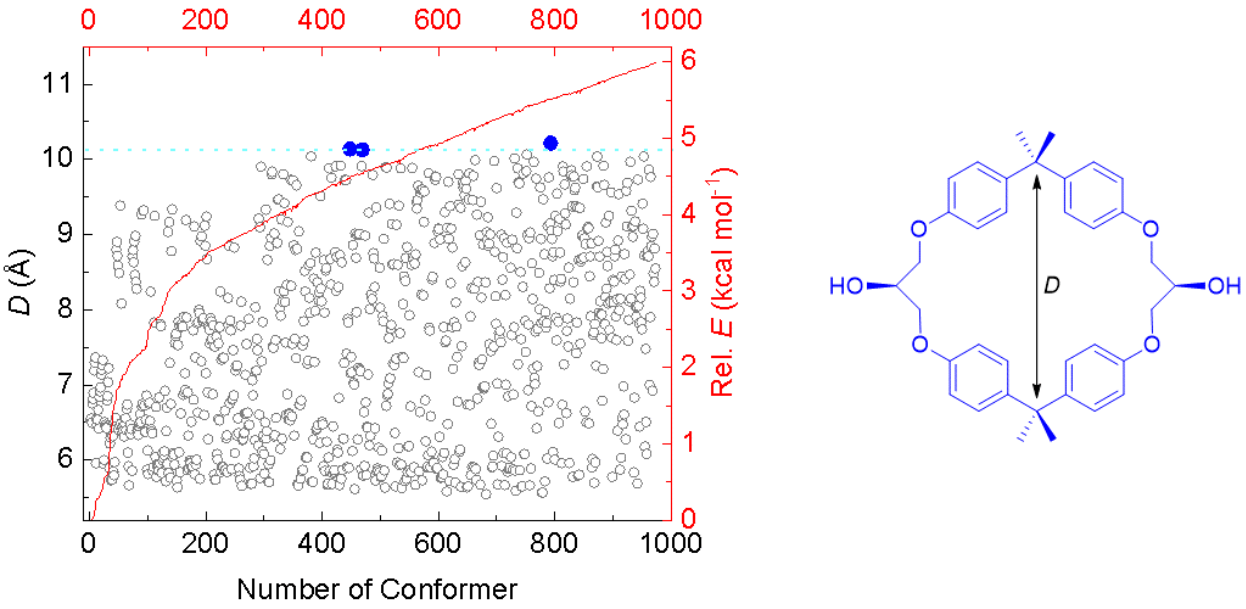

Fig. S-7 Statistical analysis of the correlations of diagonal distances (*D*) of cis cyclo-di-BADGE conformers with their relative energies (rel. *E*) based on CREST calculations.

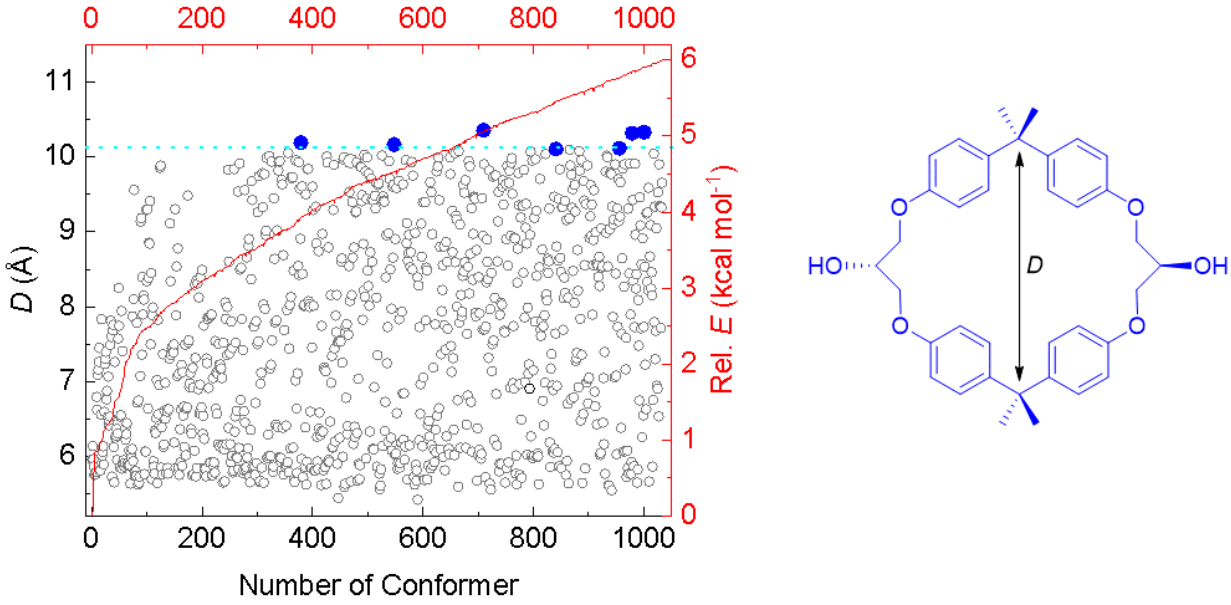

Fig. S-8 Statistical analysis of the correlations of diagonal distances (*D*) of *trans* cyclo-di-BADGE conformers with their relative energies (rel. *E*) based on CREST calculations.

Following the same CREST method, conformers of the 1:1 complexes of cyclo-di-BADGE and 4,5-pyrenedione were calculated. Fig. S-9 summarizes the *D* values of the cyclo-di-BADGE macrocycles in these conformers and their correlations with the rel. *E* of the complexes. For the 1:1 complex of *cis* cyclo-di-BADGE and 4,5-pyrenedione, there are 151 conformers predicted.

The *D* values of cyclo-di-BADGEs in these conformers range from 5.8 to 8.1 Å (see Fig. 9A). None of them shows an open-shaped cyclo-di-BADGE structure resembling that observed in the X-ray analysis. In contrast, the 1:1 complex of *trans* cyclo-di-BADGE and 4,5-pyrenedione shows 274 conformers (Fig. S-9B), in which three conformers give open-shape cyclo-di-BADGEs (*D* > 10.1 Å) resembling the X-ray structure of cyclo-di-BADGE.

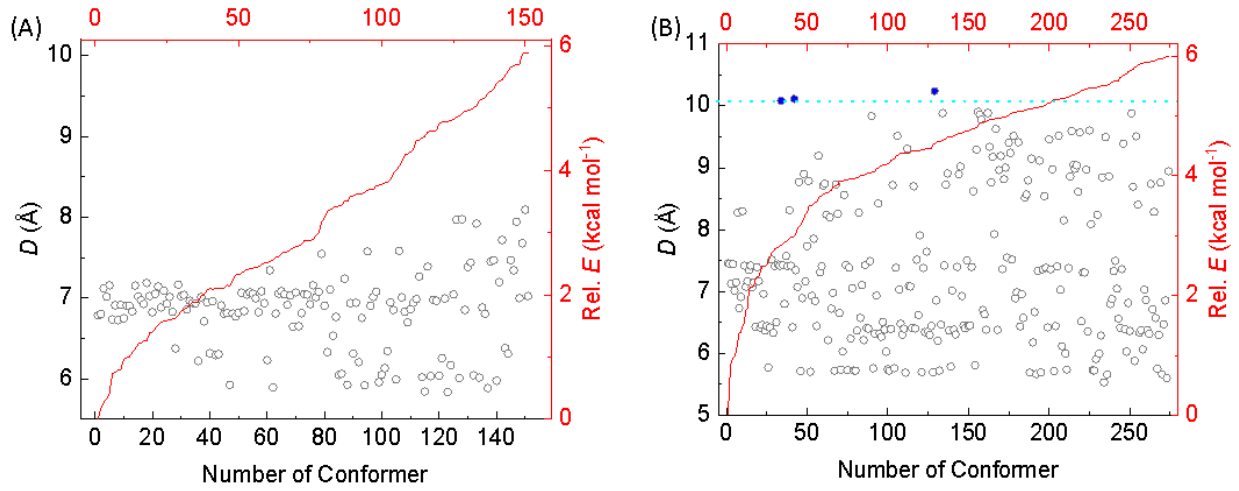

Fig. S-9 Statistical analysis of the 1:1 complexes of cylo-di-BADGE and 4,5-pyrenedione based on CREST calculations. (A) Correlations of diagonal distances (*D*) of the *cis* cyclo-di-BADGE moieties with the relative energies (rel. *E*) of the complexes. (B) Correlations of diagonal distances (*D*) of the *trans* cyclo-di-BADGE moieties with the relative energies (rel. *E*) of the complexes.

Table S-2 Summary of DFT-optimized lowest-energy folded conformers for *cis* cyclo-di-BADGE

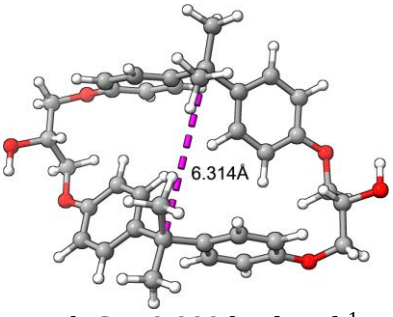 *Rel*. G = 0.000 kcal mol^{-1}	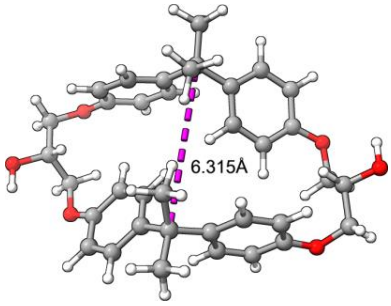 *Rel*. G = 0.175 kcal mol^{-1}	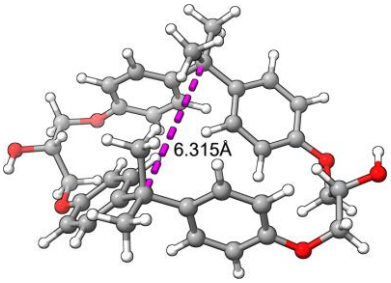 *Rel*. G = 0.242 kcal mol^{-1}
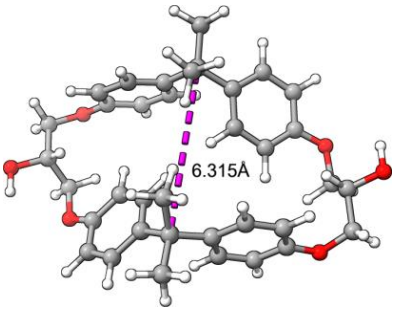 *Rel*. G = 0.264 kcal mol^{-1}	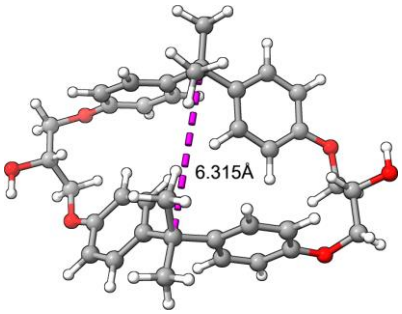 *Rel*. G = 0.332 kcal mol^{-1}	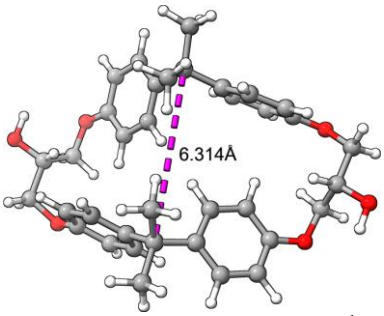 *Rel*. G = 3.180 kcal mol^{-1}

Table S-3 Summary of DFT-optimized open-shaped conformers for *cis* cyclo-di-BADGE

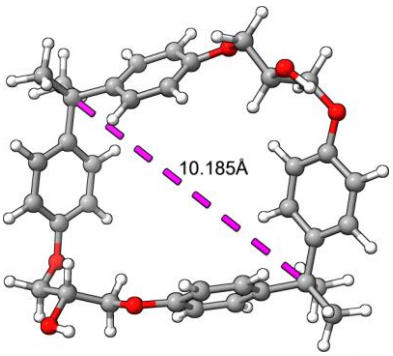 *Rel*. G = 6.341 kcal mol^{-1}	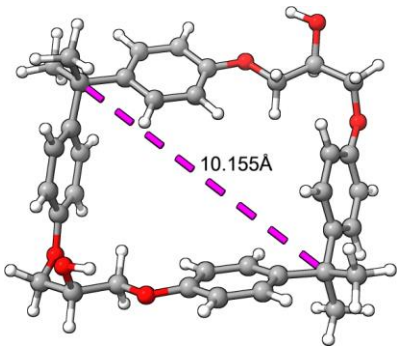 *Rel*. G = 5.536 kcal mol^{-1}	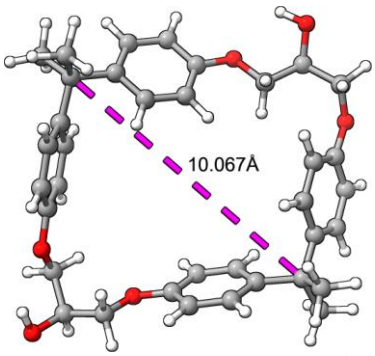 *Rel*. G = 5.590 kcal mol^{-1}

Table S-4 Summary of DFT-optimized lowest-energy folded conformers for *trans* cyclo-di-BADGE

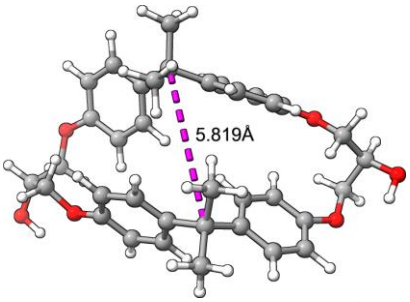 *Rel*. G = 0.000 kcal mol^{-1}	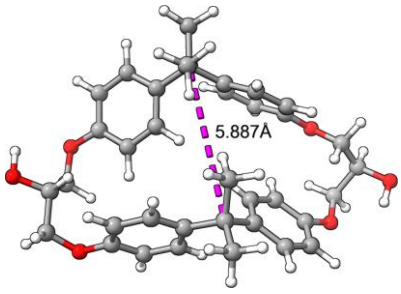 *Rel*. G = 1.068 kcal mol^{-1}	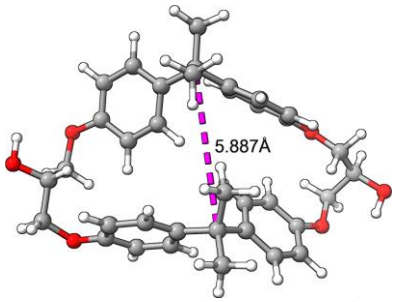 *Rel*. G = 1.072 kcal mol^{-1}
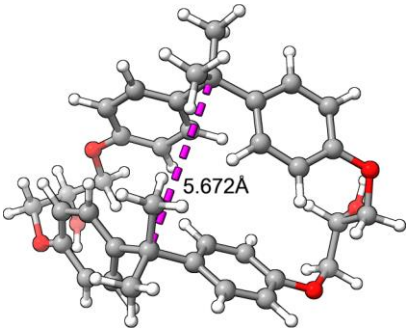 *Rel*. G = 1.268 kcal mol^{-1}	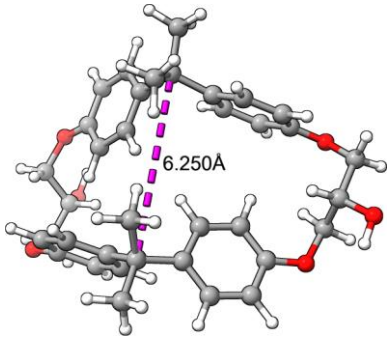 *Rel*. G = 2.345 kcal mol^{-1}	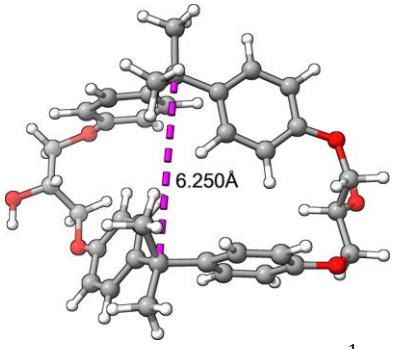 *Rel*. G = 2.346 kcal mol^{-1}

Table S-5 Summary of DFT-optimized open-shaped conformers for *trans* cyclo-di-BADGE

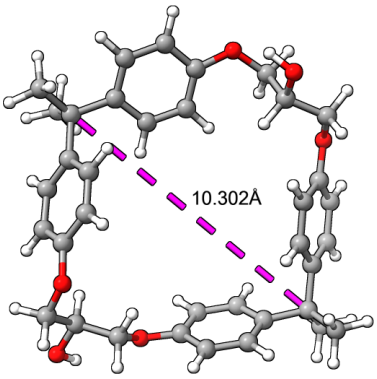 *Rel*. G = 6.647 kcal mol^{-1}	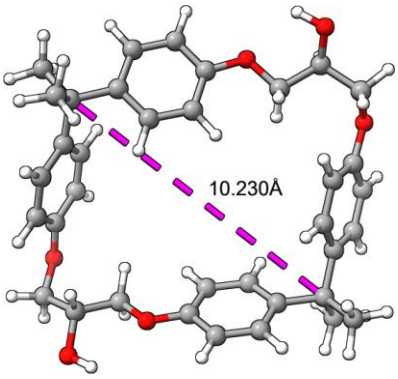 *Rel*. G = 5.602 kcal mol^{-1}	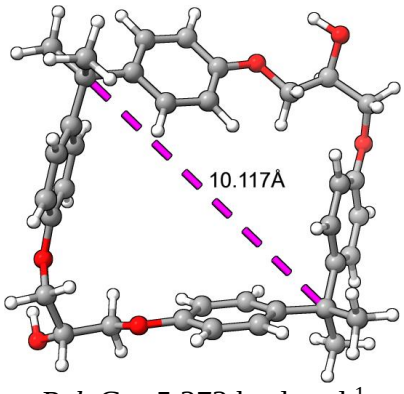 *Rel*. G = 5.373 kcal mol^{-1}

5. Results of Molecular Docking Studies

Table S-6 Docking data for stable complexes of BSA/*cis* cyclo-di-BADGE (E_b > 9.0 kcal mol^{-1})

Entry	E_b (kcal mol^{-1})	K_{diss} (10^{-6} M)	Con. Surf. (Å^2)	Contacting Receptor Residues
1	9.514	0.106	317.57	ARG194, GLN220, LYS221, VAL292, GLU93, LYS294, PRO338, GLU339, LYS439, SER442, GLU443, PRO446, CYS447, ASP450, TYR451
2	9.438	0.121	342.85	ARG217, GLN220, LYS221, GLU291, VAL292, GLU293, LYS294, PRO338, GLU339, TYR340, ALA341, VAL342, LYS439, GLU443, PRO446, CYS447, ASP450
3	9.433	0.122	343.89	ARG217, GLN220, LYS221, GLU291, VAL292, GLU293, LYS294, PRO338, GLU339, TYR340, ALA341, VAL342, LYS439, GLU443, PRO446, CYS447, ASP450
4	9.432	0.122	306.75	GLU16, GLU17, HIS18, LYS131, TRP134, ASN158, LYS159, ASN161, GLY162, GLN165, PRO281, LEU282, LEU283, GLU284
5	9.187	0.184	323.19	LEU103, SER104, HIS105, LYS106, ASP107, ASP108, SER109, TYR147, ARG196, GLN203, LYS204, VAL461, GLU464, LYS465

E_b: bing energy; K_{diss}: dissociation constant; Con. Surf.: contacting surface area.

Table S-7 Plots of stable docked complexes of BSA/*cis* cyclo-di-BADGE listed in Table S-6

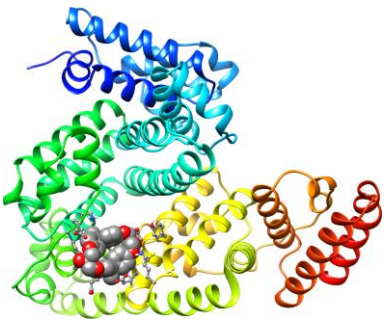 Docked complex 1	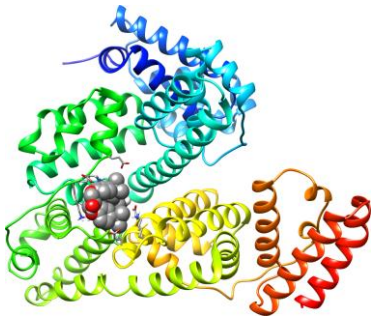 Docked complex 2	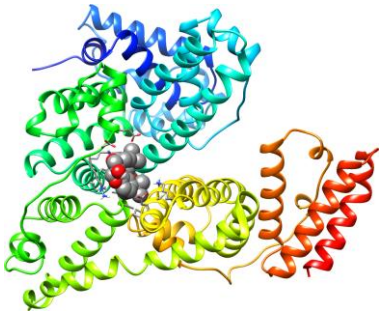 Docked complex 3
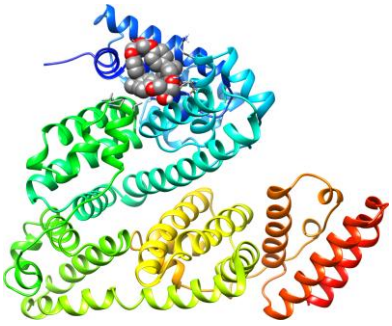 Docked complex 4	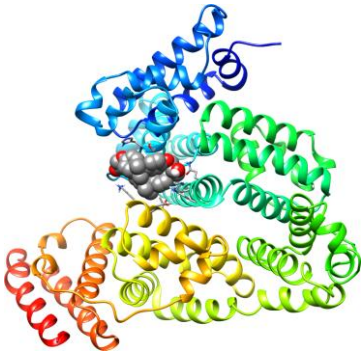 Docked complex 5	

Table S-8 Docking data for stable complexes of BSA/*trans* cyclo-di-BADGE (E_b > 9.0 kcal mol^{-1})

Entry	E_b (kcal mol^{-1})	K_{diss} (10^{-6} M)	Con. Surf. (Å^2)	Contacting Receptor Residues
1	9.918	0.054	338.46	LYS396, LEU397, GLY398, TYR400, GLY401, ASN404, ALA405, VAL408, LYS524, GLU540, LEU543, LYS544, MET547, GLU548, VAL551
2	9.171	0.189	313.72	LYS396, LEU397, GLY401, ASN404, ALA405, VAL408, LYS524, GLU540, LEU543, LYS544, MET547, GLU548, VAL551
3	9.145	0.198	318.45	LYS396, LEU397, GLY398, GLU399, TYR400, GLY401, ASN404, ALA405, VAL408, LYS524, GLU540, LEU543, LYS544, MET547, GLU548, VAL 551

E_b: bing energy; K_{diss}: dissociation constant; Con. Surf.: contacting surface area.

Table S-9 Plots of stable docked complexes of BSA/*trans* cyclo-di-BADGE listed in Table S-8

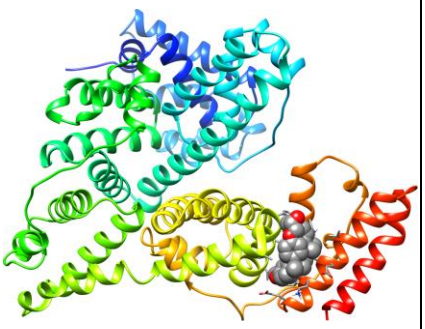 Docked complex 1	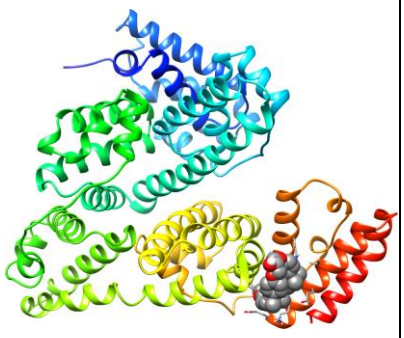 Docked complex 2	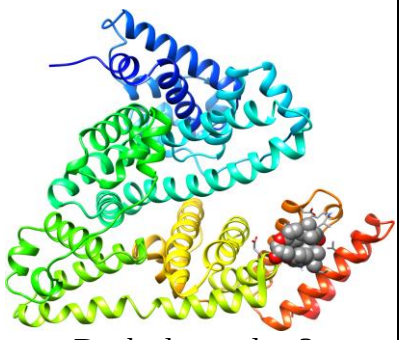 Docked complex 3